A Kinetic Model of Coordinated Myosin V†

Yudong Wu,‡ Yi Qin Gao,‡,§ and Martin Karplus*,‡,||

Department of Chemistry and Chemical Biology, Harvard University, Cambridge, Massachusetts 02138, Department of Chemistry, Texas A&M University, College Station, Texas 77845, and Laboratoire de Chimie Biophysique, ISIS, Université Louis Pasteur, 67000 Strasbourg, France

Received March 15, 2007

ABSTRACT: We present a kinetic model for the walking of myosin V on actin under conditions of zero external force. The model includes three pathways and the termination of the processivity. Experimentally measured kinetic parameters are used in the model to obtain quantitative results. Using the model and associated parameters, we compute the proportion of the pathway containing an intermediate state, as well as the walking velocities and run lengths at various concentrations of ATP and ADP. The resulting trends agree with experimental data. The model explains the surprising experimental finding that myosin walks at a faster speed but for a shorter distance as the ATP concentration increases in the absence of ADP. It also suggests that under physiological condition ([ADP] ∼ 12−50 μM), myosin walks with a higher speed and for longer distances when ATP is more abundant.

Myosin V moves processively along actin filaments (*1*, *2*), unlike conventional muscle myosin II. The processivity is essential for the fulfillment of its biological function of transporting vesicles and organelles to their destinations (*3*, *4*). One myosin V molecule has two identical heavy chains, each consisting of an N-terminal motor domain or head, a neck of six IQ motifs, and a C-terminal region or tail (*3*). The two heavy chains are joined together at the tail to form a coiled coil that is connected with a cargo-carrying globular domain. The IQ motifs provide sites by which myosin light chains or calmodulin domains bind to the heavy chains (*5*). The motor domain contains the binding sites to actin and nucleotides and catalyzes ATP[1] hydrolysis, which is a factor in controlling the motion.

As pointed out by Rosenfeld and Sweeney (*6*), myosin V is an ideal system for experimental analysis, because the rate constants for the various processes are such that they can be individually measured; e.g., P_i release is fast, unlike myosin II, where it is slow. In a recent paper (*6*), they have described a model for myosin V processivity but did not formulate it in terms of kinetic equations. Our objective is to use their data and that of others, particularly the recent work of Baker et al. (*7*) and Uemura et al. (*8*), to obtain a quantitative kinetic model for comparison with and prediction of experimental results.

During the process of movement, each motor domain experiences the same chemical cycle of binding ATP, hydrolyzing it, and releasing products (*9*−*13*). This process is activated by the presence of actin (*10*); for example, the rate of releasing ADP, which is the rate-limiting step, is increased by about a factor of 10 to ∼12−16 s^{-1} in the presence of actin (*10*). After ADP is released, ATP binds to the myosin head at a rate of 0.9 μM^{-1} s^{-1} (*10*), which leads to its dissociation from actin. ATP is then hydrolyzed, and the motor domain rebinds to actin, accompanied by the release of P_i. The system then returns to a state at which the motor domain with ADP bound is associated with actin. There appear to be several steps associated with the binding of myosin to actin (*10*), some of which are nearly irreversible. The strong tendency to form actomyosin in the absence of nucleotides, as well as in the presence of ADP, is a feature of myosin V which distinguishes it from conventional myosins, such as myosin II. This behavior is quantified by the duty ratio, the fraction of the cycle during which myosin is bound to actin (*14*−*16*). Myosin V has a high duty ratio, which is important for its function as a processive motor, since processivity requires that at least one head be attached at all times. The dissociation of myosin V from actin is triggered by the binding of ATP, which induces a conformational change in the myosin structure (*17*, *18*).

Myosin V has been shown to walk along actin as far as ∼1−2 μm and as fast as ∼0.4 μm/s by a "hand-over-hand" mechanism (*19*). The myosin molecule moves only toward the barbed end of actin. As yet the mechanism for this directionality is not understood. It has been suggested that P_i release is the controlling factor, based on single-molecule experiments with single-headed myosin V that indicate that P_i can be released only when the lever arm has a certain orientation with respect to the head (*20*). Within one cycle of ATP hydrolysis, the trailing head steps forward to pass the leading head, which remains attached to actin during this process. The trailing head advances 72 nm in one step, which results in an apparent step size of 36 nm for the center of the molecule. The step size of 36 nm (*21*, *22*), which is

† This research was supported in part by a grant from the Human Research Foundation. The parts of this study done at Harvard University were supported in part by a grant from the National Institutes of Health.

* Address correspondence to this author at Harvard University. E-mail: marci@tammy.harvard.edu. Phone: (617) 495-4018. Fax: (617) 496-3204.

‡ Harvard University.

§ Texas A&M University.

|| Université Louis Pasteur.

[1] Abbreviations: ATP, adenosine triphosphate; ADP, adenosine diphosphate.

10.1021/bi700526r CCC: $37.00
Published on Web 05/08/2007

approximately equal to the length of 13 subunits or half of a helix length of the actin filament, is much larger than that of 7−8 nm steps taken by kinesin (*23*) and those of most other myosin molecules, such as the ~5 nm step of myosin II (*24*). With this step size, the 1−2 μm processive length corresponds to 28−56 steps. The large step size is made possible by the long "lever arm", which consists of the 24 nm neck region of six IQ motifs (*21*, *22*, *25*); thus, the step size of 36 nm is a significant fraction of the 48 nm maximum. The connected lever arms also provide a mechanism for the communication of the two heads. It has been suggested (*6*) that with both heads associated with actin, the conformational change of the leading head (i.e., its reorientation with respect to actin) can be transformed into the bending of the connected lever arm, which in turn gives rise to strain in the other lever arm and its associated head. In the absence of nucleotides, a significant degree of bundling of actin filaments has been observed when myosin V binds to actin (*3*, *21*). This behavior suggests that there exists a strain between the myosin heads when both are bound to the same actin filament. The strain is apparently reduced upon the binding of ADP, as indicated by the fact that the introduction of ADP lowers the tendency toward bundling and increases the proportion of myosin that is doubly bound to the same actin filament (*21*). This result suggests that the bound conformation of the head is different in the presence and absence of ADP. Also, ADP is released from the trailing head at a rate barely double (~30 s^{-1}) that from a single-headed myosin (~16 s^{-1}), while the release from the leading head is nearly 40 times slower (0.3−0.4 s^{-1}) when both heads are associated with the same actin filament (*6*). It is likely that the strain imposed by both heads being bound to the same actin filament is the source of this difference. Evidence for the interaction between the two heads is provided by recent optical tweezer experiments, in which an external force was applied (*26*, 27).

Several kinetic schemes (*19*, *28*, *29*) that are based on a single pathway have been proposed to describe the coordination between the two heads as myosin steps along actin: Under physiological conditions ([ATP] ~ 1 mM and [ADP] ~ 0.02 mM), the rate-limiting step is the release of ADP from the trailing head when the leading head has an ADP bound and both heads are associated with actin (*2*, *19*, *28*). In these schemes, this step is followed by the binding of ATP to the trailing head, which induces its dissociation from actin. The rate constant of ATP binding is about 0.9 μM^{-1} s^{-1} (*19*, *22*, *28*), and the binding becomes rate-limiting only when [ATP] is in the submicromolar range, considerably below the physiological concentration. After ATP hydrolysis, the trailing head steps forward to become the leading head and rebinds to actin with the release of P_i. In this state, both heads of myosin are attached to actin and bind ADP. Release of ADP from the leading head is assumed to be slowed down by the strain between two lever arms. During each cycle, the leading head is assumed always to be associated with actin and to bind ADP. The scheme based on this sequence of events explains the existence of two potential rate-limiting steps at different ATP concentrations, as revealed by the single-molecule experiments (*2*, *28*). However, the scheme is not consistent with the fact that the ADP release measured from double-headed myosin in single-molecule experiments (~12−16 s^{-1}) has a rate different from those of double-headed myosin (~30 s^{-1}) by stopped-flow solution measurements (*6*), while the rate is similar to that of the release from single-headed myosin (~12 s^{-1}) (*28*, *30*). We note that these experiments are done in the presence of actin; the ADP release rate from myosin not bound to actin is 1 order of magnitude smaller (~1 s^{-1}) (*10*).

Two papers (*7*, *8*) provide data and insights essential to the present model. Baker et al. (*7*) showed that myosin walks significantly slower but takes more steps when the concentration of ATP is decreased; i.e., when [ATP] is reduced from the physiological concentration of 1 mM to 50 μM, the number of processive steps increases by more than 50%, but its speed decreases by about a factor of 4 (*7*). The step length is assumed not to change since it is determined primarily by the actin periodicity. At higher concentrations of ADP, with ATP fixed at 1 mM, myosin translocates more slowly on actin and over significantly shorter distance; for example, when [ADP] is 1 mM, in contrast to the much lower physiological concentration of [ADP] (~20 μM), myosin steps approximately 4 times more slowly and walks only half of the distance before falling off (*7*). To explain the dependence of myosin motility on the ADP concentration, Baker et al. (*7*) proposed that there are multiple kinetic pathways. Compared with the kinetic model in ref *10*, they included an additional kinetic pathway in which the release of P_i in the leading head follows the release of ADP from the trailing head. However, the modified kinetic scheme, which is based on fitting the experimental data for the ADP-dependent walking velocities and run lengths, leads to parameters which are not in agreement with other experiments; e.g., a very slow phosphate release (5 s^{-1}) is required in disagreement with the independently measured value (above 200 s^{-1}) (*10*, *30*). Also, the dependence of myosin motility on the ATP concentration is not explained by the model. Uemura et al. (*8*) identified an intermediate state in single-molecule experiments. This state corresponds to a 12 nm substep, which was followed by a 24 nm substep to reach the full-length 36 nm step. Such behavior had been observed in myosin under a load (*28*) but had not been explained in previous kinetic models. Kolomeisky and Fisher (*31*) suggested that such an intermediate state exists on the basis of the velocity−force observations by Mehta et al. (*2*). Uemura et al. (*8*) proposed an alternative kinetic model that incorporates an additional pathway with an intermediate state in which only one myosin head is associated with actin. They also suggested that an "isomerization" of the leading head with ADP bound (i.e., an unspecified conformational change) has to occur before the trailing head was able to complete its full step. This is in accord with the suggestion of Sweeney et al. (*10*) from their kinetic experiments in solution that there is more than one state of the myosin head with both ADP and actin bound. Two groups (*32*, *33*) have developed mechanochemical models to study the behavior of the lever arms and the coordination between the two heads in the presence of external forces.

In this report, we modify the kinetic model of Uemura et al. (*8*) and study the coordination between the two motor domains of myosin V during the process of walking along actin filaments under conditions of vanishing external force. This limiting case, which has been studied experimentally in some detail, is the first step in a complete model, which

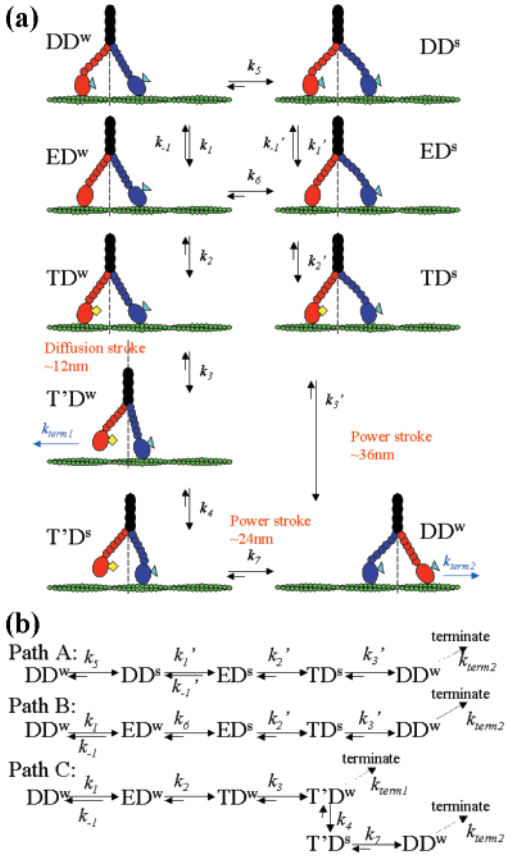

FIGURE 1: A kinetic model of how myosin V moves along actin. Each state is identified with a two-symbol code. The two letters denote the conformation of the trailing head and the leading head, respectively. Two different states of the leading head with ADP bound are included; one (D^w) binds actin weakly and the other (D^s) strongly. An intermediate state ($T'D^w$) is present in path C. (a) The overall scheme. Two heads and their connected lever arms are colored differently (in blue and red) in order to distinguish them. ADP is represented with a cyan triangle, and ATP is shown as a yellow diamond. Their relative sizes are exaggerated for vision purpose. (b) The three pathways are shown separately. The motion is terminated (denoted as "terminate" in the figure) when myosin falls off the actin filament. This can occur during the transition from TD^s (or $T'D^s$) to DD^w or at the intermediate state $T'D^w$. See text for details.

would describe the myosin kinetics in the presence of an external force. Utilizing experimentally measured parameters, we show that the proposed model is able to explain most of the existing experimental results for myosin V at zero force. Specifically, unlike the model of Baker, the present model includes an intermediate state, in analogy to that of Uemura, and shows how different rate-limiting steps arise under different solution conditions. Also, the different dependences of the motility on the concentrations of ATP and ADP observed by Baker et al. (*7*) are rationalized by the model. In addition, the observed ADP release rates are explained in a consistent fashion by the proposed model.

METHODS

(A) Kinetic Model and Parameters. The model presented in Figure 1 is used to describe the kinetics of myosin V, including the catalysis of ATP hydrolysis and the translocation along the actin filament. Our model is based upon the Uemura et al. (*8*) model. Two extra states are introduced into the pathway involving the intermediate to describe the process in more detail. More importantly, experimentally measured parameters are used in the model. In addition, inspired by the work of Baker et al. (*7*), this model describes the termination of the processivity of myosin V under different conditions.

As is evident from the figure, the kinetic model consists of eight states. A two-symbol code (DD^w, TD^w, DD^s, etc.) is used to identify the states. The first letter denotes the conformation of the trailing head and the second, the one of the leading head: E, D, and T refer to the fact that a motor domain is empty, has ADP bound, or has ATP bound, respectively. Experiments suggest that the motor domain with ADP bound has more than one conformation, although no high-resolution structures are available. A recent cryoelectron microscopy study (*34*) suggests that there is a small structural change in actin-bound myosin versus free myosin (*18*), both with ADP as a ligand. Here we make the assumption that there are two conformations for the leading head with ADP bound, D^w and D^s, where D^w and D^s are respectively weakly and strongly bound to actin. Also, recent experiments (*35*−*37*) have shown that there are two ADP states for myosin bound to actin. The trailing head is assumed to have only one conformation, denoted as D. Motor domains tend to associate with actin in the presence of bound ADP or in the absence of any bound nucleotide. Conformation E corresponds to the rigor state and is strongly bound to actin. Conformation T refers to a motor domain that has an ATP bound and is associated with actin. Kinetic data (*10*) and X-ray structures (*18*) indicate that the binding of ATP to the motor domain quickly leads to the dissociation of the motor domain from actin; the symbol T′ denotes a conformation with ATP bound but dissociated from actin. Although additional conformations of myosin V have been inferred from electron microscopy (*21*, *25*), only eight kinetically important states are included in the present model. Consequently, each "state" in the present "minimal" model can refer to several conformations in rapid equilibrium. For example, the release of P_i is very fast after hydrolysis, and this event links a state of myosin having both ADP and P_i bound with another state of myosin having only ADP bound; the state of myosin having both ADP and P_i bound is not included explicitly.

Three pathways (A, B, and C), which connect the eight states, are included in the kinetic model (see Figure 1). All of them start at state DD^w, a state with an ADP bound to both motor domains, which are both bound to actin; they are formed after ATP hydrolysis. From state DD^w, myosin V can take two possible routes, either undergoing a conformational change in the leading head (i.e., D^w to D^s) or releasing ADP from the trailing head. In the first route, denoted as path A, a conformational change of the ADP binding pocket occurs in the leading head, leading to its stronger binding to actin (state DD^s). ADP is then released from the trailing head; the strong association of the leading head (D^w to D^s) with actin leads to a conformational change in the trailing head, which is assumed to facilitate the release of ADP ($k_1' = 30\ s^{-1}$) from the trailing head (*6*). In the reverse reaction, ADP rebinds to the trailing head at a rate of $4.5\ \mu M^{-1}\ s^{-1}$ (*28*). At physiological concentrations of ADP or at the higher concentrations used in some experiments (*7*), the rate of ADP rebinding is comparable to or even larger

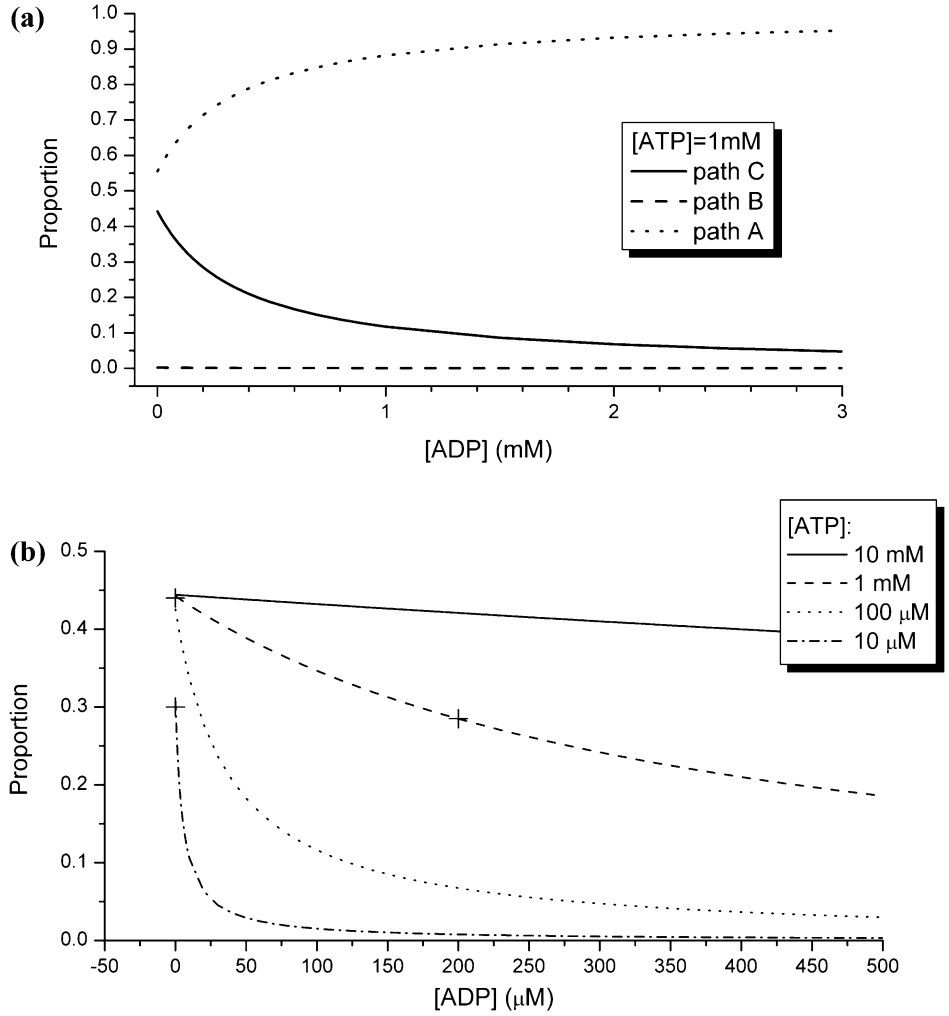

FIGURE 2: (a) Dependence of the proportions of various paths on [ADP] at [ATP] = 1 mM. Dotted, dashed, and solid lines, corresponding to the proportions of paths A, B, and C, respectively, are derived from the kinetic model. (b) Dependence of the proportion of path C on the [ADP] at various ATP concentrations. The lines are derived from the kinetic model, and three available experimental data points (*7*) are shown as crosses. The two data points at [ADP] = 0 μM, corresponding to ATP concentrations of 1 mM and 10 μM, respectively, are used to adjust kinetic parameters, k_5 and k_6, in the model. The third point at [ADP] = 200 μM and at [ATP] = 1 mM falls on the dashed line predicted by the model.

than that of ADP release. Olivare et al. (*37*) recently showed that when both heads of myosin V bind strongly to actin, the rate of ADP binding is increased from 4.5 μM^{-1} s^{-1} to approximately 13 μM^{-1} s^{-1}. Use of the latter value in the model has no effect on the path ratio, the run length, or the maximum velocity. However, the velocity would be expected to decrease somewhat faster as [ADP] increases at a given [ATP] than in the reported calculations. In the next step, ATP binds to the empty trailing head at a rate of 0.9 μM^{-1} s^{-1} (*10*, *19*, *22*, *28*) and leads to its fast dissociation (*10*) from actin. It has been shown recently (*35*, *37*) that ATP (and ADP) binding involves a two-step process; in the present model, the binding is treated as a single event with the rate constant used corresponding to the slow step. This step is immediately followed by the hydrolysis of ATP bound to the trailing head and the reorientation of the lever arm of the leading head (*10*). In this model, a power stroke occurs only when the leading head with an ADP bound is strongly associated with actin, as in the state TD^s. The power stroke (shown in Figure 1a) moves the leading lever arm in the forward direction and through the interaction with the other lever arm drives the trailing head forward. It passes by the leading head and reaches a position close to the next binding site on actin, which is approximately 36 nm ahead of where the leading head was bound. (We note that there is no substep on this pathway.) The previous trailing head with ADP and P_i bound weakly associates with actin and quickly releases P_i. The previous trailing head has now become the leading head after rebinding to the actin, and the previous leading head has become the trailing head. The cycle is complete; i.e., the system returns to the initial state DD^w.

The second and third pathways (paths B and C; see Figure 1b) start from state DD^w with ADP release from the trailing head prior to the conformational change in the leading head. In state DD^w, the leading motor domain is loosely bound to actin, and it is therefore assumed to have little effect on the release of ADP from the trailing head. Thus, the rate of this release step ($k_1 = 12$ s^{-1}) (*10*) is taken from kinetic experiments on single-headed myosin. After the release of ADP from the trailing head, the myosin molecule is in state ED^w with both heads bound to actin. At this point further branching can occur. Along path B (see Figure 2), the conformational change ($D^w \rightarrow D^s$) occurs in the leading head to form a state in which both heads are associated with actin and the leading head is strongly bound to ADP. This state (state ED^s) is also present in path A (see Figure 1b), and

from this point path B is the same as path A. The third pathway (path C; see Figure 1b) branches off from path B at state ED^w with the binding of ATP to the trailing head to give TD^w. It is also possible that myosin rebinds ADP from state ED^w at a rate of 4.5 μM^{-1} s^{-1} (*28*) and goes back to state DD^w (see also above); this possibility is included in the kinetics of both paths B and C. Along path C, myosin first binds ATP to the trailing head at a rate of 0.9 μM^{-1} s^{-1} (*10*, *19*, *22*, *28*), which is very fast (900 s^{-1}) at the physiological ATP concentration (~1 mM). The trailing head then quickly dissociates from actin (k_3 = 870 s^{-1}) (*10*). However, on this path, the conformational change has not occurred in the leading head (unlike paths A and B), and myosin is, therefore, not ready to generate a power stroke. The myosin molecule can only take a small substep (~12 nm) (*8*), corresponding to a diffusive motion, biased by the relaxation of the strain between two heads. This step introduces an intermediate state (state $T'D^w$). The intermediate state lasts until the conformational change has occurred in the leading head and the power stroke is generated. The power stroke from the leading head drives myosin forward by a substep of ~24 nm (*17*) to complete the regular step of ~36 nm. The presence of the substep in path C is clearly distinct from the stepping along paths A and B. In the latter two paths, the conformational change of the leading head occurs first, which puts strain on the trailing head. After ATP binds to the trailing head and dissociates it from actin, a full step (~36 nm) can be taken.

The lifetime of the intermediate state on path C is determined by the rate of the conformational change in the leading head. Since this conformational change does not depend on the binding of nucleotides, the external concentrations of ATP or ADP do not affect the lifetime of the intermediate state. The dwell time of the intermediate state is around 6 ms (*8*), which gives k_4 = 166 s^{-1}. Once the conformational change is completed in the leading head, the trailing head steps forward at a rate of k_7 to populate state DD^w. The constant k_7 ($T'D^s \rightarrow DD^w$) can be regarded as the rate constant of the sequential steps of ATP hydrolysis, the release of P_i, and the rebinding of the head to actin. All of these processes are very fast; e.g., the rate of releasing P_i is above 200 s^{-1}, and the other two processes are even faster (*10*, *30*). Here k_7 is assigned to be 200 s^{-1}, which is much faster than the rate of ADP release (~12−16 s^{-1}). Similarly, k_3' ($TD^s \rightarrow DD^w$) on paths A and B is the rate constant for the combined chemical reactions of ATP hydrolysis, P_i release, and the rebinding of the head to actin. It is also assigned the value of 200 s^{-1}; this is the value measured in ref *10* and is generally accepted (*30*). We note that the exact value is not critical in the present scheme because it is more than 1 order of magnitude larger than the rate of ADP release, the rate-limiting step. However, when myosin is subjected to external forces, its mechanical movement is altered dramatically and can even be smaller than the rate of the P_i release. In that case, a force-dependent rate has to be introduced for k_7 and k_3'; this is outside the scope of the present model.

(1) States of Heads with Bound ADP. Having formulated the paths that contribute to the myosin V processive cycle, we describe several of the states involved in more detail. Two conformations, D^w and D^s, are included in this model for the leading head. In both conformations, the motor domain is associated with actin; D^s is the strongly bound conformation, and D^w is a weakly bound conformation. Kinetic data show (*6*) that ADP release from the leading head is very slow (0.3−0.4 s^{-1}). This is more than 1 order of magnitude slower than the competing combined events in which the trailing head releases ADP, binds ATP, and moves forward to become the new leading head. Consequently, ADP continues to be bound to the previous leading head, which becomes the new trailing head and releases ADP much faster. This means that ADP is released only from the trailing head as double-headed myosin walks along actin. The leading head always has bound ADP so that states that are nucleotide-free or bound with ATP do not contribute. Although the states (D^w and D^s) could also exist in the trailing head, for simplicity, we consider only one conformation of the trailing head with ADP bound. Such a state, denoted as D, arises from state D^s of the leading head when the connected lever arm tilts forward. The tilt of the lever arm probably further strengthens the binding with actin and facilitates the ADP release. In summary, the trailing head can be in states D, T, T′, or E while the leading head can only be at states D^w or D^s. Since P_i release is very fast (>200 s^{-1}), we do not specifically include a state in which the leading head is bound with both products of ATP hydrolysis, ADP and P_i; such a state would be a part of D^w in the model.

(2) Termination. As myosin walks along the actin filament, one head has to detach from actin in order to move the molecule forward. When this occurs, myosin can fall off the actin track if the other head does not bind actin strongly enough. This process gives rise to the termination step in the model. As shown in Figure 1, termination can happen during the transition from TD^s (or $T'D^s$) to DD^w. This termination step has the rate k_{term2}. In addition, the intermediate state in path C, $T'D^w$, has the trailing head not bound to actin and the leading head only weakly bound. Again, there is a possibility of terminating the processivity. This termination process has the rate k_{term1} and competes with the conformational change of the leading head ($T'D^w \rightarrow T'D^s$), which leads to strong binding to actin.

The dissociation rate of ADP-bound single head myosin from actin is measured to be 0.032 s^{-1} (*10*). We take this value for k_{term1}, which is the dissociation rate from actin of the ADP-bound leading head, with the ATP binding trailing head free. The other termination rate, k_{term2}, is the dissociation rate of the leading head from actin while the trailing head is becoming detached and moving. Both heads have ADP bound and are only weakly attached to actin. Baker et al. (*7*) estimated this parameter k_{term2} to be 1.1 s^{-1}. This termination rate is an average dissociation rate of the leading head as the trailing head moves forward. The fact that the value of k_{term2} is about 30 times larger than k_{term1} is interesting and suggests that the interaction between two heads is important in the faster dissociation of the leading head from actin. We agree with Baker et al. that this is not a quantitative explanation of the difference between k_{term2} and k_{term1}; they suggest that "all the factors that contribute to termination are not fully understood yet". We note that the equilibrium constant for the association of an ADP-bound single-headed myosin to actin is 7.6 × 10^{-9} M (*10*). Such a small value suggests that the actomyosin complex is thermodynamically stable with ADP bound and supports the hypothesis that the

interaction between two ADP-bound heads is important for the termination steps.

(3) Backward Steps. As mentioned above, termination occurs at states with only one head bound to actin ($T'D^w$) or in the transition from TD^s (or $T'D^s$) to DD^w. Alternatively, the dissociation of the leading motor domain from actin could lead to a backward step, which has been observed in single-molecule studies. However, backward steps are not included in the present model because they appear to be rare; the frequencies of occurrence are not available. Backward steps are expected to be more frequent in the presence of an external force applied in the direction opposite to the myosin motion.

(B) Kinetic Equations and Parameters. On the basis of the model in Figure 1, we can write the differential equations for the time dependence of the probability of the different states during the myosin stepping cycle

$$\frac{dP_{DD^w}}{dt} = -k_1P_{DD^w} - k_5P_{DD^w} + k_{-1}P_{ED^w}[ADP] + k_7P_{T'D^s} + k'_3P_{TD^s} \quad (1a)$$

$$\frac{dP_{ED^w}}{dt} = -k_{-1}P_{ED^w}[ADP] - k_6P_{ED^w} - k_2P_{ED^w}[ATP] + k_1P_{DD^w} \quad (1b)$$

$$\frac{dP_{TD^w}}{dt} = -k_3P_{TD^w} + k_2P_{ED^w}[ATP] \quad (1c)$$

$$\frac{dP_{T'D^w}}{dt} = -k_4P_{T'D^w} + k_3P_{TD^w} \quad (1d)$$

$$\frac{dP_{T'D^s}}{dt} = -k_7P_{T'D^s} + k_4P_{T'D^w} \quad (1e)$$

$$\frac{dP_{DD^s}}{dt} = -k'_1P_{DD^s} + k'_{-1}P_{ED^s}[ADP] + k_5P_{DD^w} \quad (1f)$$

$$\frac{dP_{ED^s}}{dt} = -k'_2P_{ED^s}[ATP] - k'_{-1}P_{ED^s}[ADP] + k_6P_{ED^w} + k'_1P_{DD^s} \quad (1g)$$

$$\frac{dP_{TD^s}}{dt} = -k'_3P_{TD^s} + k'_2P_{ED^s}[ATP] \quad (1h)$$

where [ADP] and [ATP] are the concentrations of ADP and ATP, respectively.

The ratios of all these states can be determined under steady-state conditions as functions of the concentrations of ADP and ATP (see Appendix for details). This makes possible a study of the response of the behavior of myosin V to variations in [ADP] and [ATP] for given values of the kinetic parameters, which can depend on other aspects of the environment.

Two elements of the myosin behavior are of particular interest. They are the probability for myosin to take path C, denoted by r_C:

$$r_C = \frac{k_7P_{T'D^s}}{k_7P_{T'D^s} + k'_3P_{TD^s}} = \frac{k_2[ATP]}{k_2[ATP] + k_6 + \frac{k_5}{k_1}(k_{-1}[ADP] + k_2[ATP] + k_6)} \quad (2)$$

Table 1: Kinetic Parameters Used in the Model

$k_1 = 12\ s^{-1}$ [a]	$k_2 = 0.9\ \mu M^{-1}\ s^{-1}$ [a]	$k_4 = 166\ s^{-1}$ [b]
$k'_1 = 30\ s^{-1}$ [c]	$k'_2 = 0.9\ \mu M^{-1}\ s^{-1}$ [a]	$k_5 = 15\ s^{-1}$
$k_{-1} = 4.5\ \mu M^{-1}\ s^{-1}$ [a]	$k_3 = 870\ s^{-1}$ [a]	$k_6 = 4\ s^{-1}$
$k'_{-1} = 4.5\ \mu M^{-1}\ s^{-1}$ [a]	$k'_3 = 200\ s^{-1}$ [c]	$k_7 = 200\ s^{-1}$ [c]
$k_{term1} = 0.032\ s^{-1}$ [a]	$k_{term2} = 1.1\ s^{-1}$ [d]	

[a] Reference *10*. [b] Reference *8*. [c] Reference *6*. [d] Reference *7*.

and the walking velocity, V, calculated from

$$V = (k_2'P_{ED^s}[ATP] + k_2P_{ED^w}[ATP]) \times 0.036\ (\mu m) \quad (3)$$

The termination rate is too small to affect the steady state of the system as described above, so it can be introduced as a perturbation; i.e., we solve eqs 1 in its absence and use the results for the species involved to calculate the termination rate. Specifically, given the two possibilities of termination, the overall termination rate is

$$v_{term} = k_{term1}P_{T'D^w} + k_{term2}P_{DD^w} \quad (4)$$

Once the walking velocity and the termination rate are known, the run length (l) taken by myosin V before termination is equal to

$$l = V/v_{term} \quad (5)$$

Table 1 lists the parameters of the model. The value of k_{term2} is suggested by Baker's experiments (*7*). The other parameters, except for k_5 and k_6, are measured directly. The values of k_5 and k_6 were also estimated from the experimental data. Uemura et al. (*8*) found that the probability for myosin V to take path C is about 44% at 1 mM ATP, and it decreases to 30% at 10 μM ATP. At 1 mM ATP, the binding of ATP to the trailing head is very fast; k_2 is around 900 s^{-1} (1 mM $\times$ 0.9 $\mu M^{-1}\ s^{-1}$). Consequently, the system is expected to dominantly take path C from state ED^w ($ED^w \rightarrow TD^w$) instead of path B, and the probability to take path C is about $k_1/(k_1 + k_5)$; i.e., only paths A and C occur. Since we already have know $k_1 = 12\ s^{-1}$, k_5 is estimated to be $\sim$15 s^{-1}. At low concentrations of ATP (such as 10 μM), the rate of ATP binding is only about 9 s^{-1}, which makes it rate-limiting in both path A and path C. Under such a condition, the chance to take path C is reduced by the presence of path B, to $(k_1/(k_1 + k_5))(k_2[ATP]/(k_2[ATP] + k_6))$. With an ATP concentration ([ATP]) of 10 μM and the values of k_1 (12 s^{-1}), k_5 (15 s^{-1}), and k_2 (0.9 $\mu M^{-1}\ s^{-1}$), k_6 is estimated to be about 4 s^{-1}. In our model, the rear head is still attached, but the ligation state is different (in A with ADP bound and in B it is empty), so it is not unreasonable that the constants should not be the same. From the model, if the trailing head is more strongly bound, the isomerization of the leading head is slower.

(C) Comparison of Models. To make clear the significance of the present model, we summarize the differences between it and earlier work.

Uemura et al. (*8*) established experimentally that myosin V can follow two distinct pathways, one with a (12 + 24) nm substructure and the other with no detectable intermediate in a 36 nm step. They also included a step linking these two distinct pathways. In this step, the leading head undergoes a conformational change (from D* to D) while the trailing head is not associated with nucleotides. We treat the process

involving this step as an additional path. Thus, our model has three pathways. There are six states in the model of Uemura et al. with two pathways, while our model has eight states and three pathways. Also, Uemura et al. did not work out the kinetics of their conceptual model, while in our case the rates are determined. In addition, we introduce termination steps into the model, which were not included by Uemura et al. Independently, Baker et al. (*7*) studied myosin V in detail under zero load and measured run lengths and velocity under varying [ATP], [ADP], and [P_i]. They did propose a detailed kinetic model, but it is significantly different from our model. In their model, there are many substeps but no intermediate state like T′D^w in our model. For example, Baker et al. suggest that the conformational change at the leading head drags the molecule ahead for 12 nm and the dissociation of ADP from the trailing head fuels another 6 nm advance. This does not agree with the experimental results of Uemura et al., who found experimentally that the intermediate dwell time is independent of [ATP] and [ADP]. This indicates that there is a substep not coupled with ADP release. We follow the model of Uemura et al. in this respect and include a substep only for an intermediate state independent of [ATP] and [ADP]. Because of the lack of more explicit data, we adopt the description by Baker et al. for termination by introducing it into an overall kinetic step from state DD^w.

We use many kinetic parameters given in refs *6* and *10* by Sweeney et al. The first paper focused on the kinetics of single-head myosin. The second paper built a model for a double-headed myosin and described three pathways, two of which lead to termination and only one is concerned with precession. In our model, we follow the approach of Baker et al. to use simplified termination steps and expand the precession cycle to three pathways following Uemura et al. Thus, the present model is based on ideas and data from the work of Sweeney and Rosenfeld, Uemura et al., and Baker et al. It uses essential elements from each paper to construct a kinetic analysis that describes all of the available zero force data for myosin V in a consistent manner.

RESULTS

In this section, we use the model described above to study the steady-state dependence of the motility of myosin on the concentrations of ADP and ATP. The walking velocity and the run length, as well as the proportion of path C, are considered. The values of the parameters, as listed in Table 1, are taken mainly from experiments with [KCl] = 50 mM except that k_4 is measured at 75 mM KCl and k_{term2} is measured at 100 mM KCl. These concentrations of KCl have been used in many experiments, although the physiological [KCl] is between 100 and 200 mM. Baker et al. (*7*) show that K_M of myosin (i.e., [ATP] at half-maximum velocity) is 6.1 ± 1.1 μM at [KCl] = 25 mM and 163 ± 21 μM at [KCl] = 100 mM (*7*). Thus the parameters could change under other experimental conditions, and the results given here have to be interpreted accordingly. In addition, Sakamoto et al. (*38*) showed that run length drops significantly with an increase in [KCl]; e.g., the mean run lengths are 2.39 and 0.66 μm when [KCl] equals 150 and 400 mM, respectively. However, the walking velocity reaches a plateau of ~1 μm/s when [KCl] is about 150 mM (*38*). Given these dependencies, we focus primarily on the trends of the variations of the run length and velocity on [ADP] and on [ATP] instead of specific values. We compare directly with experiments where possible.

Effect of ADP on Myosin Activity. We study here the effect of ADP on r_C, on the walking velocity, and on the run length. We single out path C because it is the one that has an intermediate state and can be studied directly by experiment. As shown in eq 2, the proportion of path C depends on the concentrations of both ADP and ATP.

The increase of [ADP] shifts the balance between DD^w and ED^w toward the former so that the proportion of path A increases (Figure 2a). However, the change in [ADP] has only a small effect on the proportion of path B. Consequently, at 1 mM [ATP] or less, the proportion of path C decreases significantly as [ADP] increases, as shown in Figure 2a.

Figure 2b shows r_C as a function of ADP concentration. In the absence of ADP, r_C is around 0.44 at [ATP] = 1 mM, and its value changes little when [ATP] is between 100 μM and 10 mM. When ATP is present at high concentrations (10 mM), the proportion decreases by about 10% (from 0.444 to 0.39) as [ADP] increases from 0 to 500 μM. However, when ATP is present at low concentrations (10 μM), the proportion of path C drops dramatically (from 0.308 to 0.157) with a small increase of [ADP] from 0 to 5 μM. Under the physiological condition ([ATP] = 1 mM; the dashed line in Figure 2a), the calculated proportion varies from 0.39 to 0.43 with values of [ADP] within the physiological range (between 12 and 50 μM). The proportion decreases to 0.186 at [ADP] = 500 μM. Uemura et al. (*19*) found that the proportion is about 0.28 at 200 μM ADP and 1 mM ATP. From the kinetic model (as shown in Figure 2a), the proportion is 0.285, in excellent agreement with experiment (*8*). It would be very helpful to have additional data here for more detailed tests of the model.

ADP inhibition of the motility of myosin is well documented by experiment (*13*). Panels a and b of Figure 3 show the dependence of the walking velocity and run length, respectively, of myosin on [ADP]. ADP is calculated to moderately inhibit the movement of myosin under physiological conditions ([ATP] ~ 1 mM, [ADP] ~ 12−50 μM); i.e., both the velocity and the run length decrease with increasing [ADP]. The inhibition becomes dramatically greater as [ATP] decreases or [ADP] increases. In Figure 3a, at both ATP concentrations, even when [ADP] is similar to [ATP], myosin continues to walk more slowly as [ADP] increases, and it finally approaches zero velocity. Interestingly, as seen from Figure 3b, even when the velocity approaches zero, myosin walks a nearly constant distance before falling off. This surprising result, consistent with experimental observations (*7*), is explained by the kinetic model, in which the increase of [ADP] has two consequences. First, ADP is more competitive in rebinding to the nucleotide-free head, so that states DD^w and DD^s are more populated. Myosin is therefore more likely to take path A, which does not have an intermediate state with a termination branch such as in path C, leading to a smaller termination rate. Second, more frequent rebinding of ADP slows down the apparent dissociation of ADP from DD^w and DD^s, as well as the overall walking velocity. Quantitatively, the reduction of the walking velocity is more significant than the effect on the termination. Consequently, the run length, i.e., the ratio of the walking velocity to the termination rate,

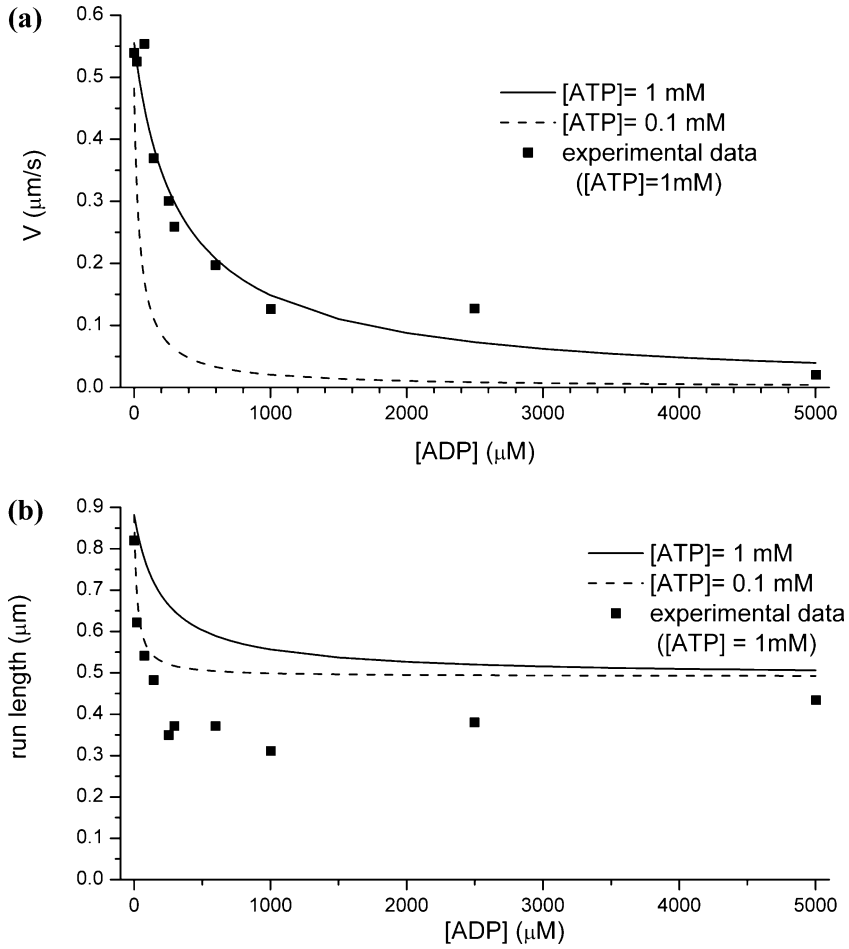

FIGURE 3: Walking velocity and run length of myosin. The *x*-axis is the ADP concentration. Two ATP concentrations, 1 and 0.1 mM, are used in the kinetic model to derive solid and dotted lines in the figures. As [ADP] increases to infinity, the velocity and the run length converge to 0 μm/s and 0.49 μm, respectively, using the parameters in Table 1. Experimental data are taken from Figure 3 in ref *7*. They are measured at 1 mM ATP and 100 mM KCl; the model is for [KCl] = 75 mM (see text). (a) Dependence of the walking velocity of myosin on [ADP]. The walking velocity predicted from the model is in excellent agreement with the experimental data. (b) Dependence of the run length of myosin on [ADP]. The run length agrees qualitatively with the experimental observations; i.e., the run length drops significantly with the increase in [ADP] when it is smaller than 300 μM and changes little when [ADP] is larger than 300 μM. The disagreement in the limiting values is probably due to the values of the termination rate constants, which are not known very accurately (see text).

follows the decrease in the velocity as [ADP] increases. Under the limiting condition of high [ADP] (greater than millimolar), almost all myosin molecules take path A (see Figure 2b), which has a velocity and a termination rate independent of nucleotide concentration (see Figure 1b). The walking velocity is approximately k_5 times the DD^w concentration, and the termination rate is k_{term2} times the DD^w concentration. The run length is, therefore, a constant, (k_5/k_{term2}) $\times$ 0.036 μm. This result shows that, even under extreme inhibition by ADP, myosin is able to walk a fixed distance before termination although it walks extremely slowly.

Effect of ATP on Myosin Activity. The dependence of the proportion of path C on [ATP] is shown in Figure 4. We note that a logarithm scale is used for [ATP]; this is different from the linear scale used for [ADP] in Figures 2 and 3. With the increase of [ATP], path C increases in importance relative to path B since the binding of ATP to the trailing head becomes faster. The distribution between paths B and C depends on the ratio of two rates: the isomerization rate of the leading head when the nucleotide-free trailing head is associated with actin ($ED^w \rightarrow ED^s$) and the rate of ATP binding ($ED^w \rightarrow TD^w$). The former is 4 s^{-1}, independent of [ATP], and the latter is proportional to [ATP]. Thus, more molecules are calculated to take path C as [ATP] increases. In the physiological (millimolar) range, the ATP binding rate is around 900 s^{-1}, which is significantly larger than the 4 s^{-1} isomerization rate, so that under these conditions, few molecules take path B; i.e., the proportion of path C reaches a limiting value of 0.44 in the physiological [ATP] range, with path B making essentially no contribution. As [ADP] increases, the nucleotide-free trailing head is more likely to bind ADP to re-form state DD^w and redistribute into the different paths so that the proportion of path C decreases as shown in Figure 4. Specifically, the proportion of path A increases. Figure 5 shows that, at the absence of ADP, the proportion of path A is a constant ($\sim$0.56); it is determined by k_1 and k_5. In the presence of ADP, the proportion of path A is no longer a constant. It starts high at low [ATP]; e.g., the value at 1 μM ATP reaches unity and converges to 0.56 at high [ATP]. In addition, at various concentrations of ADP, the limiting values of paths B (0.0) and C (0.44) are the same, but there is a variation in the ATP concentrations at which these limits are reached. For example, the proportion of path C reaches its limiting value at 400 μM ATP in the absence of ADP and in the physiological ([ATP] $\sim$mM)

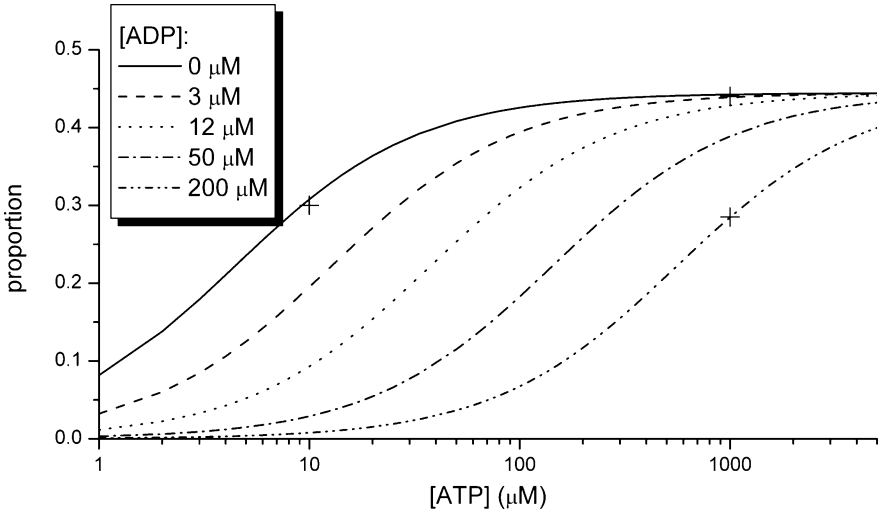

FIGURE 4: Dependence of the proportion of path C (the probability for myosin to take path C) on the concentration of ATP at different ADP concentrations. The *x*-axis is the ATP concentration, plotted on a logarithm scale, and the *y*-axis is the probability for myosin to take path C. The lines are derived from the kinetic model and correspond to different ADP concentrations. With the increase of [ATP], the proportion of path C reaches a limiting value of 0.44 regardless of [ADP]. Three experimental data points are shown as crosses. The two data points at [ADP] = 0 μM were used in estimating parameters, k_5 and k_6. The third point at [ADP] = 200 μM and [ATP] = 1000 μM is a prediction of the model.

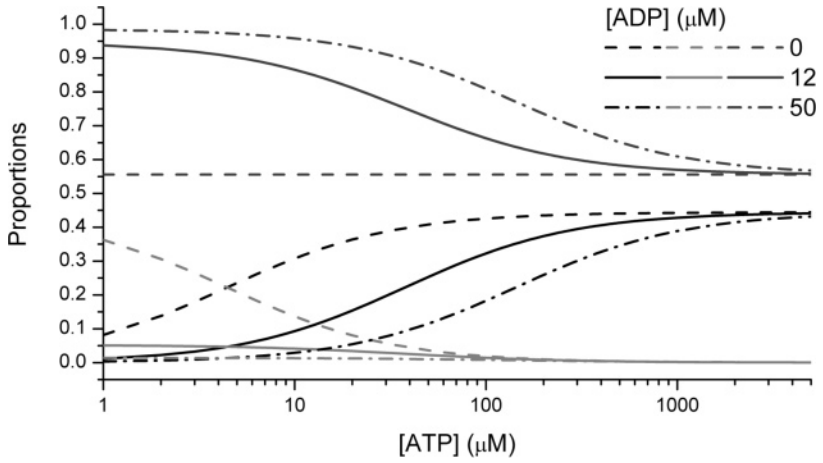

FIGURE 5: Dependence of the contributions of paths A, B, and C on the ATP concentration. The *x*-axis is the ATP concentration plotted on a logarithm scale, and the *y*-axis corresponds to the probability for myosin to take various paths. The lines are derived from the kinetic model at various [ADP]: the solid, dashed, and dotted lines correspond to ADP concentrations of 0, 12, and 200 μM, respectively. With the increase of [ATP], the proportions of paths A, B, and C reach limiting values of 0.55, 0.0, and 0.44, independent of [ADP].

range in 12 μM ADP. In the presence of 200 μM ADP, path C does not reach the limit in the physiological range of [ATP].

Figure 6 shows the myosin motility on a function of [ATP] for a series of different values of [ADP]; we note that both [ATP] and the velocity are plotted on a reciprocal scale in the panels. Figure 6a shows that the walking velocity of myosin satisfies Michaelis−Menten kinetics regardless of the value of [ADP]. Given the parameters in Table 1, the K_M values are different (17, 47, and 136 μM, respectively) at three different [ADP] (0, 12, and 50 μM), but V_{max} is the same (0.56 μm/s). When ATP is abundant (i.e., the concentration is above 50 μM) myosin takes either path A or path C. In addition, it is found to be dominantly in state DD^w (58%) or DD^s (29%). The maximum walking velocity is then given by $0.58(k_5 + k_1) \times 0.036$ μm/s, where 0.58 is the population of state DD^w, k_5 and k_1 are the rates of leaving state DD^w in paths A and C, respectively (see Figure 1), and 0.036 μm is the step size. At physiological conditions, [ADP] is within the range of 12 and 50 μM, and the corresponding K_M is between 47 and 136 μM, significantly lower than the millimolar concentration of ATP at physiological conditions. The walking velocity is, therefore, close to V_{max}, 0.56 μm/s, and it is not strongly affected by the variation of [ADP] within the physiological range. From Figure 6a, the walking velocity is calculated to be between 0.48 and 0.53 μm/s. However, when ATP is deficient, the variation of [ADP] can have a dramatic inhibiting effect on the walking velocity. For example, at [ATP] = 10 μM (1/[ATP] = 0.1 μM^{-1}) and [ADP] between 0 and 50 μM, [ATP] is below K_M, and the walking velocity is expected to be below half of V_{max}. From Figure 6a, the walking velocity is calculated to have a range of 0.03−0.21 μm/s.

Figure 6b shows the dependence of the run length on [ATP] at the same physiological values of [ADP] as used in Figure 6a. Interestingly, although at all [ADP] the walking velocities monotonically increase as [ATP] increases (see Figure 6a), the run lengths show different patterns for various [ADP]: as [ATP] increases, the run length is essentially constant in the absence of ADP, and it increases at physi-

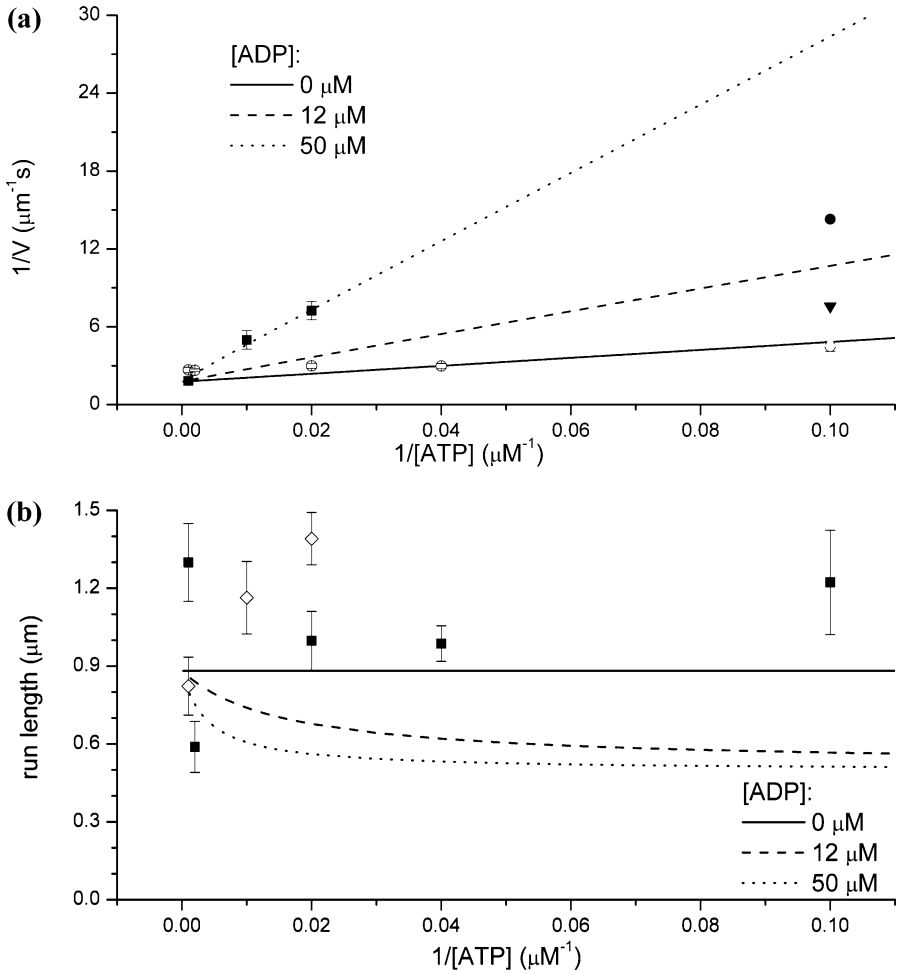

FIGURE 6: Dependence of the myosin motility on the ATP concentration calculated from the model. The *x*-axis is the reciprocal of [ATP] in both figures. (a) The reciprocal of the velocity corresponding to three different [ADP]. The solid line corresponds to [ADP] = 0 μM, the dashed line to [ADP] = 12 μM, and the dotted line to [ADP] = 50 μM. The latter two correspond to two bounds of the physiological [ADP]. These three lines satisfy Michaelis−Menten kinetics corresponding to the equation $1/V = (1/V_{max})(1 + K_M/[ATP])$ with V_{max} = 0.56 μm/s; the K_M values are 17, 47, and 136 μM for [ADP] = 0, 12, and 50 μM, respectively. (b) Run lengths at three different ADP concentrations. The three curves correspond to [ADP] = 0 (solid), 12 (dashed), and 50 (dotted) μM. The three curves converge to 0.882 μm as 1/[ATP] approaches 0. In both figures, data points and their associated error bars are experimental data taken from the same experiment (Figure 2 in ref *7*). Data points are measured at 100 mM KCl and 25 mM KCl, respectively; the ADP concentrations were not given. In panel a, some additional experimental data points are shown: one point is taken from ref *2*; another point is taken from ref *28*; another is taken from ref *8*.

ological concentrations ([ADP] = 12−50 μM). From eqs 3−5 and eq A3 in the Appendix, the run length l can be shown to be

$$l = \frac{V}{v_{term}} = \frac{(k_2' P_{EDs}[ATP] + k_2 P_{EDw}[ATP]) \times 0.036\ (\mu m)}{k_{term1} P_{T'Dw} + k_{term2} P_{DDw}} = \frac{k_5 k_{-1}[ADP] + k_5 k_6 + k_1 k_6 + (k_1 + k_5) k_2 [ATP]}{k_{term2}(k_{-1}[ADP] + k_6) + (k_{term1} k_1 / k_4 + k_{term2}) k_2 [ATP]} \times 0.036\ (\mu m) \quad (6)$$

When 1/[ATP] approaches 0 or, in other words, [ATP] → ∞, the run length has the limiting value:

$$l_{[ATP]\to\infty} = \frac{k_1 + k_5}{k_{term1} k_1 / k_4 + k_{term2}} \times 0.036\ (\mu m) \quad (7)$$

The limiting value is independent of [ADP]. Thus, in Figure 6b, the three lines converge to the same point, 0.882 μm, as ATP → ∞. At the other limit, when [ATP] approaches 0, the run length has the limit

$$l_{[ATP]\to 0} = \frac{k_5 k_{-1}[ADP] + k_5 k_6 + k_1 k_6}{k_{term2}(k_{-1}[ADP] + k_6)} \times 0.036\ (\mu m) \quad (8)$$

This limiting value depends on [ADP]. In the absence of ADP, it reaches an upper bound, $(k_5 + k_1)/k_{term2} \times 0.036$ (μm). This upper limit is 0.884 μm, marginally larger than $l_{[ATP]\to\infty}$; i.e., the run length is nearly constant (see Figure 6b). When [ADP] is very high, $l_{[ATP]\to 0}$ reaches a lower bound, $l_{[ATP]\to 0} = k_5/k_{term2} \times 0.036$ (μm). This limiting value, 0.491 μm, is lower than the limiting value as [ATP] approaches infinity, $l_{[ATP]\to\infty}$, under the condition that $k_{term2}/k_{term1} > k_5/k_4$. In such a situation, the run length decreases as 1/[ATP] increases. Under physiological conditions ([ADP] = 12−50 μM), the run length decreases as 1/[ATP] increases, as shown in Figure 6b. At a certain value of [ADP], 0.159 μM, the run length is essentially independent of [ATP]. The run length shows the largest variation with [ADP] when ATP is deficient; i.e., $l_{[ATP]\to 0}$ varies between 0.491

and 0.884 μm. In the presence of more ATP, the variation of the run length over the entire range of [ADP] becomes smaller; in the limit of large [ATP], the run length is 0.884 μm, independent of [ADP]. In the physiological range ([ATP] ~mM, [ADP] ~12−50 μM), the run length varies between 0.80 and 0.86 μm.

In experiments, a wide range of K_M values have been measured for double-headed myosin as a function of [KCl]; e.g., 6.1 μM (*7*) and 11.7 μM (*22*) at 25 mM KCl, 0.15 μM (*11*) at 80 mM KCl, and 163 μM (*7*) at 100 mM KCl; the low value measured at 80 mM KCl is surprising. The kinetic model predicts that K_M values are sensitive to the environment; they vary from 17 to 136 μM when [ADP] changes only from 0 to 50 μM. Thus, it is possible that variations in [ADP] are, in part, responsible for the apparent [KCl] dependence. However, the experimental value of V_{max} has less variation: 0.38 μm/s at 25 mM KCl (*7*), 0.453 μm/s at 80 mM KCl (*22*), and 0.55 μm/s at 100 mM KCl (*7*). These results are consistent with what are predicted in Figure 6a: V_{max} is insensitive to the environment, and its value is 0.56 μm/s. The walking velocity 0.3−0.5 μm/s found in most experiments (*2*, *7*, *8*, *17*, *24*, *28*) at the physiological conditions covers the range predicted from the model (0.48−0.53 μm/s). At low concentration of [ATP], the walking velocity measured in experiments has a very wide range (0.07−0.22 μm/s) (*2*, *7*, *8*, *28*). The model suggests that such a wide range of the walking velocity measured at low concentration of [ATP] could be due to the different [ADP] present in the system. We note that different experimental conditions and procedures could also contribute to the range of in vitro motor velocities measured in different laboratories.

Some experimental data corresponding to 100 and 25 mM KCl are shown in Figure 6a (see legend). The kinetic model shows that ATP binding becomes faster with an increase in [ATP]. This increases the overall stepping rate along all paths and thus the movement of myosin. As predicted from the model, the walking velocity is observed to increase when [ATP] increases. Interestingly, the experimental data measured at 100 mM KCl are close to the prediction at the condition of 50 mM KCl and 50 μM ADP. The experimental data measured at 25 mM KCl are close to those predicted values based on 50 mM KCl and 0 μM ADP.

The experimental data shown in Figure 6b indicate that the run length increases when 1/[ATP] increases at 100 mM KCl. Such a trend is not evident at 25 mM KCl. The kinetic model with parameters in Table 1, however, suggests that the run length decreases when 1/[ATP] increases at 100 mM KCl. In addition, the run length measured in the physiological condition ([ATP] ~mM, [ADP] ~12−50 μM) is 1−2 μm (*2*, *38*), slightly different from 0.80−0.86 μm as predicted from the model. We note that the run length depends on the condition of the measurements and any values of termination rates used in the model; the results are sensitive, in particular to k_{term2}, which has not been measured and so was estimated (see above). Taking into account the potential interaction between two heads, the dissociation rate of single-headed myosin from actin, 0.032 s^{-1}, is likely to be a lower bound for the true value. Even if this lower bound is used, the run length would be around 30 times longer. On the other hand, backward steps are neglected in our model. If backward steps are taken into consideration, the run length will be shorter. Overall, the run length is not expected to be more than 1 order of magnitude larger than estimated.

We note that Robblee et al. (*35*) suggest that the maximum rate is achieved at [ADP] ~ 200 μM or [ATP] ~ 2 mM. However, Baker et al. (*7*) show that the rate increases when [ADP] is above 200 μM. Such discrepancy may be due to the fact that single-headed myosin is used in the experiment of Robblee et al. but double-headed myosin is used by Baker et al.

CONCLUDING DISCUSSIONS

Overview. We have described a kinetic model for the coordinated walking of myosin V under zero external force. The model has three pathways, one of which contains an intermediate state, as suggested by Uemura et al. (*8*). Using the model and the associated parameters, we compute the proportion of the pathway with an intermediate state at various concentrations of ATP and ADP, and the result trends agree with the available measurements. The walking velocity under physiological condition ([ATP] ~mM) calculated from the model is consistent with the data. In addition, the model suggests that the wide range of walking velocities measured at low [ATP] is probably due to inhibition by ADP. This provides a reconciliation of the large differences in experimental measurements. These predictions should be tested by more controlled experiments. Extension of the model to include, for example, the calcium dependence of myosin V behavior (*37*) would also be of interest.

Another important aspect of the model is that it describes the termination of the processivity of myosin V, which is not included in the Uemura et al. (*8*) model, for example. This makes it possible to explain the fact that the walking velocity and the run length decrease as the ADP concentration increases (*7*). Furthermore, the model shows that myosin walks at a higher speed but for a shorter distance as [ATP] increases in the absence of ADP. This result is in accord with observations, but is not explained by other models (*7*). Also, under physiological conditions ([ADP] ~ 12−50 μM), myosin is calculated to walk at a faster speed and for a longer distance when [ATP] increases.

The present model is largely based on experimental observations, and although it is simple, it explains most of the existing experimental results. More complex models could be introduced, although it appears that they are not necessary for the explanation of the present data. More measurements, such as the run lengths at various [ATP], [ADP], and [KCl] would be helpful in determining the required rate parameters and would provide a better understanding of the termination mechanism. Measurements under substantial external loads would make it possible to extend the model to include other phenomena, such as back-stepping and slippage. Such additional experiments could also be used to distinguish the present model from other alternatives.

Coordination between Two Heads. The duty ratio from single-headed myosin experiments is useful for understanding the processivity of myosin V. However, the coordination between two heads is important to accurately adjust the relative timing of the binding; i.e., one myosin head is bound to actin while the other one is free. The present kinetic model makes it possible to study the coordination. It explains the fact that myosin walks faster but its run length is slightly

shorter at higher [ATP] and that myosin walks slower at lower [ADP] but it does not stop. These results arise from a precise coordination between two heads and the existence of multiple pathways.

Intramolecular strain is one way for two heads of myosin to communicate, as discussed by Rosenfeld and Sweeney (*6*). Its existence is confirmed by the presence of two distinct ADP-releasing rates from two-headed myosin in solution. The one of the trailing head is facilitated (30 s^{-1}) (*6*) while the one at the leading head is hindered (0.3−0.4 s^{-1}) (*6*), as compared with the release of ADP from a single-headed myosin (∼12 s^{-1}) (*6*). An assumption in the model is that two different states (D^W and D^S) are present when ADP is bound to myosin attached to actin. This has been suggested by a previous experiment (*10*) but lacks direct proof. Under this assumption, the leading head with ADP bound has two states with different affinities for actin. Its state directly affects the rate of ADP release from the trailing head through intramolecular strain. The state DD^w is generated by P_i release, and the leading head binds to actin weakly. State DD^s, in which ADP binds the leading head more strongly, arises from the isomerization of DD^w or the binding of myosin with ADP to actin in solution. The strong binding of the leading head to actin facilitates the dissociation of ADP from the trailing head. Therefore, 30 s^{-1}, the rate of ADP release from the trailing head after myosin with ADP bound to both heads associates with actin in solution, can be assigned to k'_1, the ADP release from state DD^s. In a single-molecule experiment, ADP may be released directly from the trailing head when it is in state DD^w, or the release can occur following the isomerization at the leading head. The rate in the first case is k_1 (12 s^{-1}); the limiting rate in the second case is 15 s^{-1}. These values are consistent with what has been repeatedly measured in various single-molecule experiments for ADP release (12−15 s^{-1}) (*2*, *23*, *28*).

Besides the impact of the state of the leading head on the release of ADP from the trailing head, our model includes another example of the coordination between two heads via "intramolecular strain": the state of the trailing head affects the isomerization of the leading head. In the model, the conformational change of the leading head (i.e., the isomerization from D^w to D^s) can occur under three different conditions: from DD^w to DD^s, from ED^w to ED^s, and from $T'D^w$ to $T'D^s$. In the first two cases, the trailing head is bound to actin, while in the last case the trailing head is detached. The model suggests that the strong binding of the trailing head onto actin reduces the isomerization speed of the leading head: in the last case, since the trailing head has already become released from actin and is ready to move further forward, the conformational change of the leading head (166 s^{-1}) is 1 order of magnitude faster than that if the trailing head is still bound to actin, whether ADP is bound (15 s^{-1}) or not (4 s^{-1}).

Biological Implications. Living systems have to be able to respond to perturbed conditions or different physiological requirements. When the concentrations of ATP and/or ADP fluctuate, myosin V can continue to fulfill its biological function. The finding that the motility of myosin is insensitive to the fluctuation of [ATP] around the physiological level demonstrates the stability of the walking mechanism. However, the strong dependence of the motility of myosin V on the ADP concentration suggests that the movement of myosin can be finely tuned. This leads to a sensitive control mechanism because [ADP] is much lower than [ATP] under physiological condition.

When the system is low on [ATP] or exposed to high [ADP], myosin V is more likely to take path B or path A, both of which have a higher probability of processivity. In this way, the system utilizes the limited energy source more efficiently. This suggests a possible mechanism for adaptation of the system to changes in the environment. Under limiting conditions (i.e., when the system is under extreme ATP starvation or under extreme inhibition by ADP) myosin V is still able to move processively although it moves very slowly. In this way, the cargo carried by myosin V will eventually reach to its destination instead of getting lost.

APPENDIX

After a sufficiently long reaction time (e.g., more than five cycles of the slowest step), the distribution over all states reaches a steady state so that

$$\frac{dP_{XY}}{dt} = 0 \tag{A1}$$

where XY refers to all of the states in the model (DD^w, ED^w, TD^w, $T'D^w$, DD^s, ED^s, TD^s, $T'D^s$). In addition, the system must be at some state, that is

$$P_{DD^W} + P_{ED^W} + P_{TD^W} + P_{T'D^W} + P_{DD^S} + P_{ED^S} + P_{TD^S} + P_{T'D^S} = 1 \tag{A2}$$

From (1), (A1), and (A2), the distributions over all states at the steady state are

$$P_{ED^W} = 1/\left[\frac{(k_5B + k_1k_6)}{k_1}\left(\frac{k_2'[ATP] + k_{-1}'[ADP]}{k_1'k_2'[ATP]} + \frac{1}{k_2'[ATP]} + \frac{1}{k_3'}\right) + k_2[ATP]\left(\frac{1}{k_3} + \frac{1}{k_4} + \frac{1}{k_7}\right) - \frac{k_6}{k_1'} + \frac{B}{k_1} + 1\right]$$

$$P_{DD^W} = (B/k_1)P_{ED^W}$$

$$P_{TD^W} = (k_2[ATP]/k_3)P_{ED^W}$$

$$P_{T'D^W} = (k_2[ATP]/k_4)P_{ED^W}$$

$$P_{T'D^S} = (k_2[ATP]/k_7)P_{ED^W}$$

$$P_{DD^S} = \left[\frac{k_5B + k_1k_6}{k_1[ATP]}\left(\frac{k_2'[ATP] + k_{-1}'[ADP]}{k_1'k_2'}\right) - \frac{k_6}{k_1'}\right]P_{ED^W}$$

$$P_{ED^S} = [(k_5B + k_1k_6)/(k_1k_2'[ATP])]P_{ED^W}$$

$$P_{TD^S} = [(k_5B + k_1k_6)/(k_1k_3')]P_{ED^S} \tag{A3}$$

where $B = k_{-1}[ADP] + k_6 + k_2[ATP]$.

ACKNOWLEDGMENT

The authors thank Profs. H. L. Sweeney and S. S. Rosenfeld for helpful discussions.

REFERENCES

1. Titus, M. A. (1997) Motor proteins: Myosin V—The multi-purpose transport motor, *Curr. Biol. 7*, 301−304.

2. Mehta, A. D., Rock, R. S., Rief, M., Spudich, J. A., Mooseker, M. S., and Cheney, R. E. (1999) Myosin-V is a processive actin-based motor, *Nature 400*, 590−593.
3. Cheney, R. E., O'Shea, M. K., Heuser, J. E., Coelho, M. V., Wolenski, J. S., Espreafico, E. M., Forscher, P., Larson, R. E., and Mooseker, M. S. (1993) Brain myosin-v is a 2-headed unconventional myosin with motor-activity, *Cell 75*, 13−23.
4. Wu, X., Bowers, B., Rao, K., Wei, Q., and Hammer, J. A. (1998) Visualization of melanosome dynamics within wild-type and dilute melanocytes suggests a paradigm for myosin V function in vivo, *J. Cell Biol. 143*, 1899−1918.
5. Espindola, F. S., Suter, D. M., Partata, L. B., Cao, T., Wolenski, J. S., Cheney, R. E., King, S. M., and Mooseker, M. S. (2000) The light chain composition of chicken brain myosin-Va: Calmodulin, myosin-II essential light chains, and 8-kDa dynein light chain/PIN, *Cell Motil. Cytoskeleton 47*, 269−281.
6. Rosenfeld, S. S., and Sweeney, H. L. (2004) A model of myosin V processivity, *J. Biol. Chem. 279*, 40100−40111.
7. Baker, J. E., Krementsova, E. B., Kennedy, G. G., Armstrong, A., Trybus, K. M., and Warshaw, D. M. (2004) Myosin V processivity: Multiple kinetic pathways for head-to-head coordination, *Proc. Natl. Acad. Sci. U.S.A. 101*, 5542−5546.
8. Uemura, S., Higuchi, H., Olivares, A. O., De La Cruz, E. M., and Ishiwata, S. (2004) Mechanochemical coupling of two substeps in a single myosin V motor, *Nat. Struct. Mol. Biol. 11*, 877−882.
9. Trybus, K. M., Krementsova, E., and Freyzon, Y. (1999) Kinetic characterization of a monomeric unconventional myosin V construct, *J. Biol. Chem. 274*, 27448−27456.
10. De La Cruz, E. M., Wells, A. L., Rosenfeld, S. S., Ostap, E. M., and Sweeney, H. L. (1999) The kinetic mechanism of myosin V, *Proc. Natl. Acad. Sci. U.S.A. 96*, 13726−13731.
11. Wang, F., Chen, L., Arcucci, O., Harvey, E. V., Bowers, B., Xu, Y., Hammer, J. A., II, and Sellers, J. R. (2000) Effect of ADP and ionic strength on the kinetic and motile properties of recombinant mouse myosin V, *J. Biol. Chem. 275*, 4329−4335.
12. De La Cruz, E. M., Wells, A. L., Sweeney, H. L., and Ostap, E. M. (2000) Actin and light chain isoform dependence of myosin V kinetics, *Biochemistry 39*, 14196−14202.
13. De La Cruz, E. M., Sweeney, H. L., and Ostap, E. M. (2000) ADP inhibition of myosin V ATPase activity, *Biophys. J. 79*, 1524−1529.
14. Howard, J. (1997) Molecular motors: structural adaptations to cellular functions, *Nature 389*, 561−567.
15. Veigel, C., Wang, F., Bartoo, M. L., Sellers, J. R., and Molloy, J. E. (2001) The gated gait of the processive molecular motor, myosin V, *Nat. Cell Biol. 4*, 59−65.
16. Smith, D. A. (2004) How processive is the myosin-V motor?, *J. Muscle Res. Cell Motil. 25*, 215−217.
17. Holmes, K. C., Angert, I., Kull, F. J., Jahn, W., and Schröder, R. R. (2003) Electron cryo-microscopy shows how strong binding of myosin to actin releases nucleotide, *Nature 425*, 423−427.
18. Coureux, P. -D., Sweeney, H. L., and Houdusse, A. (2004) Three myosin V structures delineate essential features of chemo-mechanical transduction, *EMBO J. 23*, 4527−4537.
19. Yildiz, A., Forkey, J. N., McKinney, S. A., Ha, T., Goldman, Y. E., and Selvin, P. R. (2003) Myosin V walks hand-over-hand: Single fluorophore imaging with 1. 5-nm localization, *Science 300*, 2061−2065.
20. Watanabe, T. M., Tanaka, H., Iwane, A. H., Maki-yonekura, S., Homma, K., Inoue, A., Ikebe, R., Yanagida, T., and Ikebe, M. (2004) A one-headed class V myosin molecule develops multiple large (approximate to 32-nm) steps successively, *Proc. Natl. Acad. Sci. U.S.A. 101*, 9630−9635.
21. Walker, M. L., Burgess, S. A., Sellers, J. R., Wang, F., Hammer, J. A., III, Trinick, J., and Knight, P. J. (2000) Two-headed binding of a processive myosin to F-actin, *Nature 405*, 804−807.
22. Forkey, J. N., Quinlan, M. E., Shaw, M. A., Corrie, J. E. T., and Goldman, Y. E. (2003) Three-dimensional structural dynamics of myosin V by single-molecule fluorescence polarization, *Nature 422*, 399−404.
23. Svoboda, K., Schmidt, C. F., Schnapp, B. J., and Block, S. M. (1993) Direct observation of kinesin stepping by optical trapping interferometry, *Nature 365*, 721−727.
24. Mehta, A. D., Finer, J. T., and Spudich, J. A. (1997) Detection of single-molecule interactions using correlated thermal diffusion, *Proc. Natl. Acad. Sci. U.S.A. 94*, 7927−7931.
25. Burgess, S., Walker, M., Wang, F., Sellers, J. R., White, H. D., Knight, P. J., and Trinich, J. (2002) The prepower stroke conformation of myosin V, *J. Cell Biol. 159*, 983−991.
26. Veigel, C., Schmitz, S., Wang, F., and Sellers, J. R. (2005) Load-dependent kinetics of myosin-V can explain its high processivity, *Nat. Cell Biol. 7*, 861−869.
27. Purcell, T. J., Sweeney, H. L., and Spudich, J. A. (2005) A force-dependent state controls the coordination of processive myosin V, *Proc. Natl. Acad. Sci. U.S.A. 102*, 13873−13878.
28. Rief, M, Rock, R. S., Mehta, A. D., Mooseker, M. S., Cheney, R. E., and Spudich, J. A. (2000) Myosin-V stepping kinetics: A molecular model for processivity, *Proc. Natl. Acad. Sci. U.S.A. 97*, 9482−9486.
29. Vale, R. D. (2003) Myosin V motor proteins: marching stepwise towards a mechanism, *J. Cell Biol. 163*, 445−450.
30. Mehta, A. (2001) Myosin learns to walk, *J. Cell Sci. 114*, 1981−1998.
31. Kolomeisky, A. B., and Fisher, M. E. (2003) A simple kinetic model describes the processivity of myosin-V, *Biophys. J. 84*, 1642−1650.
32. Lan, G., and Sun, S. X. (2005) Dynamics of myosin-V processivity, *Biophys. J. 88*, 999−1008.
33. Vilfan, A. (2005) Elastic lever-arm model for myosin V, *Biophys. J. 88*, 3792−3805.
34. Volkmann, N., Liu, H., Hazelwood, L., Krementsova, E. B., Lowey, S., Trybus, K. M., and Hanein, D. (2005) The structural basis of myosin V processive movement as revealed by electron cryomicroscopy, *Mol. Cell 19*, 595−605.
35. Robblee, J. P., Cao, W., Henn, A., Hannemann, D. E., and De La Cruz, E. M. (2005) Thermodynamics of nucleotide binding to actomyosin V and VI: a positive heat capacity change accompanies strong ADP binding, *Biochemistry 44*, 10238−10249.
36. Hannemann, D. E., Cao, W., Olivares, A. O., Robblee, J. P., and De La Cruz, E. M. (2005) Magnesium, ADP, and actin binding linkage of myosin V: evidence for multiple myosin V-ADP and actomyosin V-ADP states, *Biochemistry 44*, 8826−8840.
37. Olivares, A. O., Chang, W., Mooseker, M. S., Hackney, D. D., and De La, Cruz, E. M. (2006) The tail domain of myosin Va modulates actin binding to one head, *J. Biol. Chem. 281*, 31326−31336.
38. Sakamoto, T., Amitani, I., Yokota, E., and Ando, T. (2000) Direct observation of processive movement by individual myosin V molecules, *Biochem. Biophys. Res. Commun. 272*, 586−590.

BI700526R